Int. J. Solids Structures, Vol. 11, pp. 1367–1380. Pergamon Press 1975. Printed in Great Britain

TRAVELING WAVES VIBRATIONS AND BUCKLING OF ROTATING ANISOTROPIC SHELLS OF REVOLUTION BY FINITE ELEMENTS

JOSEPH PADOVAN†
University of Akron, Akron, OH 44325, U.S.A.

(*Received* 2 *May* 1975; *revised* 27 *May* 1975)

Abstract—A quasi-analytical finite element procedure is developed which can obtain the frequency and buckling eigenvalues of prestressed rotating anisotropic shells of revolution. In addition to the usual centrifugal forces, the rotation effects treated also include the contribution of Coriolis forces. Furthermore, since a nonlinear version of Novoshilov's shell theory is employed to develop the element formulation, the effects of moderately large prestress deflection states can be handled. Due to the generality of solution procedure developed, the axisymmetric prestress states treated can also consist of torque loads. In order to illustrate the procedures capabilities, as well as the significant effects of Coriolis forces, torque prestress and material anisotropy, several numerical experiments are presented.

INTRODUCTION

The problem of free vibrations and buckling of shells under the influence of prestress fields has stimulated considerable attention. Numerous recent numerical investigations have taken advantage of the capacities of current generation computers to analyze more accurate models of shell structures. For shells of revolution as well as more general geometries, such investigations have reached a high level of generality as witnessed in the mature works of references[1–6].

In spite of the comprehensive capabilities of presently available finite element schemes for shells of revolution, the quasi-analytical formulations still have several important shortcomings outstanding. For instance, the prestressed free vibration and buckling versions are as yet limited to orthotropic stationary shells subject to torsionless prestress states. Hence, the important effects of material anisotropy[7–9], torque prestress[9–10] and Coriolis forces[9, 11–12] are completely neglected. Furthermore, the problem of traveling flexural waves induced by moving loads in prestressed structures has also been neglected from the computational point of view. The critical velocity of such waves, which marks the transition from subcritical to supercritical wave forms, is of importance for design purposes in several prestressed aerospace and commercial structures (tires[13, 14] and turbines, etc.) and hence, needs further attention.

In the context of the foregoing, the present work will extend the quasi-analytical version of the finite element procedure to handle free vibrations, critical circumferential traveling wave velocities and stability problems of shells of revolution incorporating such effects as; (i) Coriolis forces; (ii) axisymmetric torque prestress states and; (iii) material anisotropy. Since the effects of moderate prestress deflections are considered, following the works of Cohen[2] and Bushnell[4], a nonlinear version of Novoshilov's[15] shell theory will be used to set up the requisite pertubational finite element formulation including the effects of (i–iii) noted above. As will be seen later, due to the inclusion of (i–iii), the governing field equations take on a noncanonical form which prevents the usage of the classical quasi-analytical procedures employed by[1–4]. For the present work, this difficulty is circumvented in the manner of[16]. Since this procedure leads to a complex regular polynomial matrix problem, the complex eigenvalue procedure developed by Gupta[17] can be used to obtain the requisite eigenvalues. For the stability problem, complex versions of the eigenvalue procedures employed by Bushnell[4], and Cohen[2] are discussed. In order to establish the requisite eigenvalue problem for the critical circumferential traveling wave velocities, the Galilean coordinate shift[18] is used to transform the governing equations of motion into the appropriate standing wave problem. After finite

†Associate Professor of Mechanical Engineering.

element modelling, the resulting eigenvalue problem is complex, hence, the procedure of Gupta[17] is also used to evaluate the critical wave speeds.

In the sections to follow, discussions are given on; (1) governing shell theory employed; (2) pertubational finite element approximation; (3) perturbational finite element field equations; (4) critical circumferential traveling wave eigenvalue problem; (5) eigenfunction and eigenvalue properties and; (6) discussion of results. In order to illustrate the potential of the quasi-analytical finite element procedure derived herein, as well as the importance of items (i–iii), several numerical experiments are also included. These will give comparisons with the works of previous investigators.

2. GOVERNING SHELL THEORY

As noted in the introduction, the shell formulation adopted herein is a nonlinear version of Novoshilov's theory[15]. For the general case of shells composed of heterogeneous anisotropic composite media, the requisite constitutive law takes the form

$$\{\sigma\} = [D]\{\epsilon\} \tag{1}$$

such that

$$\{\sigma\}^T = \{T_1, T_2, \tilde{T}_{12}, M_1, M_2, \tilde{M}_{12}\} \tag{2}$$

$$\{\epsilon\}^T = \{\epsilon_1, \epsilon_2, \epsilon_{12}, \kappa_1, \kappa_2, \kappa_{12}\} \tag{3}$$

and the material stiffness matrix $[D]$ is defined by

$$[D] = \begin{bmatrix} A_{11} & A_{12} & A_{13} & B_{11} & B_{12} & B_{13} \\ & A_{22} & A_{23} & B_{12} & B_{22} & B_{23} \\ & & A_{33} & B_{13} & B_{23} & B_{33} \\ & & & D_{11} & D_{12} & D_{13} \\ \text{Symmetrical} & & & & D_{22} & D_{23} \\ & & & & & D_{33} \end{bmatrix} \tag{4}$$

where the individual elements of $[D]$ are given by

$$\begin{aligned} \langle A_{ab}, B_{ab}, D_{ab}\rangle &= \langle E_{ab}(1, z, z^2)\rangle;\ a, b = 1, 2 \\ \langle A_{a3}, B_{a3}, D_{a3}\rangle &= \langle E_{a4}(1, z, z^2)\rangle;\ a = 1, 2 \\ \langle A_{33}, B_{33}, D_{33}\rangle &= \langle E_{44}(1, z, z^2)\rangle \end{aligned} \tag{5}$$

with

$$\langle\ \rangle = \int_{-h}^{h} (\ )\,\mathrm{d}z \tag{6}$$

The E_{ab} elements appearing in eqn (5) represent the actual 3-D material stiffnesses. Following Novoshilov's shell resultant convention, $\tilde{T}_{12}$ and $\tilde{M}_{12}$ appearing in eqn (2) are defined by

$$\begin{aligned} \tilde{T}_{12} &= T_{12} - M_{21}/R_2 = T_{21} - M_{12}/R_1 \\ \tilde{M}_{12} &= (M_{12} + M_{21})/2 \end{aligned} \tag{7}$$

As moderately large deformations are assumed, in order to establish the requisite stability and vibration equations, $\{\epsilon\}$ is taken as

$$\begin{Bmatrix} \epsilon_1 \\ \epsilon_2 \\ \epsilon_3 \\ \epsilon_4 \\ \epsilon_5 \\ \epsilon_6 \end{Bmatrix} = \begin{Bmatrix} e_1 \\ e_2 \\ e_{12} \\ \kappa_1 \\ \kappa_2 \\ \kappa_{12} \end{Bmatrix} + (1/2) \begin{Bmatrix} \chi & \beta & 0 \\ 0 & \beta & \psi \\ \psi & 0 & \chi \\ 0 & 0 & 0 \\ 0 & 0 & 0 \\ 0 & 0 & 0 \end{Bmatrix} \begin{Bmatrix} \chi \\ \beta \\ \psi \end{Bmatrix} \tag{8}$$

such that $e_1, \ldots$ and $\kappa_1, \ldots$ have the form

$$\begin{Bmatrix} e_1 \\ e_2 \\ e_{12} \end{Bmatrix} = \begin{Bmatrix} (r/R_2)\xi' + r'\eta' \\ (1/r)(v^{\cdot} + \eta) \\ \xi^{\cdot}/R_2 + (r'/r)\eta^{\cdot} + v' - r'/(rR_1)v \end{Bmatrix} \tag{9}$$

$$\begin{Bmatrix} \kappa_1 \\ \kappa_2 \\ \kappa_{12} \end{Bmatrix} = \begin{Bmatrix} \chi' \\ (1/r)(((r'/r)\xi - \eta/R_2)^{\cdot\cdot} + v^{\cdot}/R_2 + r'\chi) \\ (r'/r)\xi^{\cdot\prime} - \eta^{\prime\cdot}/R_2 - (r'/r)^2\xi^{\cdot} + r'/(rR_2)\eta^{\cdot} + v'/R_1 - r'/(r/R_2)v \end{Bmatrix} \tag{10}$$

$$\begin{Bmatrix} \psi \\ \beta \\ \chi \end{Bmatrix} = \begin{Bmatrix} v/R_2 - (r'/r)\xi^{\cdot} + \eta^{\cdot}/R_2 \\ (r'/r)v + \xi^{\cdot}/R_2 + (r'/r)\eta^{\cdot} \\ r'\xi' - (r/R_2)\eta' \end{Bmatrix} \tag{11}$$

The displacement components ξ and η appearing in eqns (9)–(11) are the global counterparts (Fig. 1) of u and w as defined by the relation

$$\begin{Bmatrix} u \\ w \end{Bmatrix} = \begin{bmatrix} r/R_2 & r' \\ -r' & r/R_2 \end{bmatrix} \begin{Bmatrix} \xi \\ \eta \end{Bmatrix} \tag{12}$$

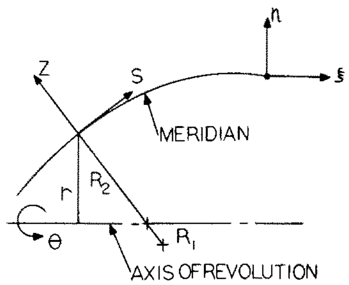

Fig. 1. Axial section of shell of revolution.

3. PERTURBATIONAL FINITE ELEMENT APPROXIMATIONS

As was pointed out recently by[16], the appearance of the A_{13}, A_{23}, B_{13}, B_{23} and D_{13}, D_{23} elements of the material stiffness matrix for the anisotropic case results in a noncanonical form for the governing field equations and therefore prevents the traditional[1–4] application of Fourier decomposition. Interestingly, this same difficulty is also caused by the allowance of axisymmetric torque prestress fields for both stability and free vibration analyses[8]. For this reason, previous stability and free vibration procedures have been restricted to axisymmetric torsionless prestress fields which admit the traditional usage of Fourier decomposition[8, 9, 16].

As the stability and free vibration properties of small perturbations about the general axisymmetric prestress fields of rotating anisotropic shells are sought, the displacements ξ, η and v are taken in the form

$$\{Y(s,\theta,t)\} = \begin{Bmatrix} \xi(s,\theta,t) \\ \eta(s,\theta,t) \\ v(s,\theta,t) \end{Bmatrix} \simeq \{Y_0(s)\} + \{Y_p(s,\theta,t)\} \tag{13}$$

In order to circumvent the difficulties noted earlier, the exact removal of the θ variable from the governing field equations is obtained by seeking $\{Y_p\}$ in the form[16]

$$\{Y_p\} = \sum_{m=-\infty}^{\infty} \{Y_{mp}\} e^{jm\theta} \tag{14}$$

such that $j = \surd(1)$ and

$$\{Y_{mp}\} = (1/2\pi)\int_0^{2\pi} \{Y_p\} e^{-jm\theta} \, d\theta \tag{15}$$

Now, in terms of eqns (13) and (14), $\{Y\}$ at any point within the eth element can be approximated by

$$\{Y\}^e \sim [N]^e\{Y_0\}^e + \sum_{m=-\infty}^{\infty} [N_m]^e\{Y_{mp}\}^e \, e^{jm\theta} \tag{16}$$

where the shape functions $[N]^e$ and $[N_m]^e$ have the following partitioned forms:

$$[N]^e = [N_i[I], \ldots]^e \tag{17}$$

$$[N_m]^e = [N_{mi}[I], \ldots]^e \tag{18}$$

The nodal displacements $\{Y_0\}^e$ and $\{Y_{mp}\}^e$ appearing in eqn (16) are defined by

$$(\{Y_0\}^e)^T = \{\xi_{0i}, \eta_{0i}, v_{0i}, \xi_{0k}, \eta_{0k}, v_{0k}, \ldots\}^e \tag{19}$$

$$(\{Y_{mp}\}^e)^T = \{\xi_{mpi}, \eta_{mpi}, \omega_{mpi}, \xi_{mpk}, \eta_{mpk}, v_{mpk}, \ldots\}^e \tag{20}$$

such that $\xi_{mpi}, \eta_{mpi}, \ldots$ represent the complex perturbational nodal displacements and $i, k, \ldots$ denote the nodes associated with the eth element.

In terms of eqn (16), assuming that $\|\{Y_p\}\| \ll 1$ for all $s \epsilon S$, the shell strain relations, eqns (3) and (8)–(11), can be rewritten as

$$\{\epsilon\}^e \sim \{\epsilon_0\}^e + \sum_{m=-\infty}^{\infty} [[B_{mp}] + [B_{0n}][G_{mp}]]^e\{Y_{mp}\}^e \, e^{jm\theta} + (1/2) \sum_{m=-\infty}^{\infty} \sum_{M=-\infty}^{\infty} [B_{mpn}]^e[G_{Mp}]^e\{Y_{Mp}\}^e \, e^{j(m+M)\theta} \tag{21}$$

where the coefficients matrices $[B_{0n}]^e$, $[B_{mp}]^e$, $[G_{mp}]^e$ and $[B_{mpn}]^e$ have the following partitioned forms:

$$([B_{0n}]^e)^T = \begin{bmatrix} \chi_0 & 0 & \psi_0 & 0 & 0 & 0 \\ \beta_0 & \beta_0 & 0 & 0 & 0 & 0 \\ 0 & \psi_0 & \chi_0 & 0 & 0 & 0 \end{bmatrix}^e \tag{22}$$

$$[B_{mp}]^e = [B_{mpi}, B_{mpk}, \ldots]^e \tag{23}$$

$$[G_{mp}]^e = [G_{mpi}, G_{mpk}, \ldots]^e \tag{24}$$

$$([B_{mpn}]^e)^T = \begin{bmatrix} \chi_{mp} & 0 & \psi_{mp} & 0 & 0 & 0 \\ \beta_{mp} & \beta_{mp} & 0 & 0 & 0 & 0 \\ 0 & \psi_{mp} & \chi_{mp} & 0 & 0 & 0 \end{bmatrix} \tag{25}$$

For convenience, the various partitions making up eqns (22)–(25) are given in the appendix. Due to the use of the complex form of Fourier series, namely eqn (14), the various partitions of $[B_{mp}]^e$ $[G_{mp}]^e$, $[B_{mpn}]^e$ and $\{Y_{mp}\}^e$ satisfy the following conjugate property, namely,

$$([\bar{B}_{mp}], [\bar{G}_{mp}], [\bar{B}_{mpn}], \{\bar{Y}_{mp}\})^e = ([B_{-mp}], [G_{-mp}], [B_{-mpn}], \{Y_{-mp}\})^e \tag{26}$$

such that the overbar denotes complex conjugation. Since material anisotropy and torque prestress are admitted herein, the present description of $\{\epsilon\}$ includes such prestress field variables as β_0, ψ_0 and v_0 which are neglected in traditional orthotropic torsionless formulations. These effects are represented in the various partitions of $[B_{0n}]$, $[B_{mpn}]$ and $[G_{mp}]$ as given in the Appendix.

4. PERTURBATIONAL FINITE ELEMENT FIELD EQUATIONS

Since the present work considers the analysis of a conservative holonomic gyroscopic system, the effects of Coriolis forces as well as torque prestress and material anisotropy are admitted. Hence, accounting for the moving frame of reference, the usual virtual work expression takes the following more general form, namely,

$$\int_0^{2\pi}\int_S ((\delta\{\epsilon\})^T\{\sigma\}+(\delta\{Y\})^T\{[\alpha_1]\{Y\}_{,tt}+\Omega[\alpha_2]\{Y\}_{,t}+\Omega^2[\alpha_3]\{Y\}\})\,r\,ds\,d\theta=0 \tag{27}$$

where the various mass matrices $[\alpha_i]$; $i=1, 2, 3$ appearing in eqn (27) are given by

$$[\alpha_1]=\langle\rho\rangle[H]^T[I][H] \tag{28}$$

$$[\alpha_i]=\langle\rho\rangle[H]^T[\alpha_{i+2}][H];\ i=2,3 \tag{29}$$

such that

$$[\alpha_4]=2\begin{bmatrix}0 & r' & 0\\ -r' & 0 & r/R_2\\ 0 & -r/R_2 & 0\end{bmatrix} \tag{30}$$

$$[\alpha_5]=\begin{bmatrix}-(r')^2 & 0 & rr'/R_2\\ 0 & -1 & 0\\ rr'/R_2 & 0 & (r/R_2)^2\end{bmatrix} \tag{31}$$

$$[H]=\begin{bmatrix}r/R_2 & r' & 0\\ 0 & 0 & 1\\ -r' & r/R_2 & 0\end{bmatrix} \tag{32}$$

and Ω is the rotational speed of the shell. Unlike $[\alpha_1]$ which is positive definite, $[\alpha_i]$; $i=2, 3$ have indefinite quadratic forms.

In terms of eqn (21), $\delta\{\epsilon\}^e$ appearing in eqn (27) is given by

$$\delta\{\epsilon\}^e\sim\sum_{m=-\infty}^{\infty}\left\{[[B_{0n}][G_{mp}]+[B_{mp}]]^e\delta\{Y_{mp}\}^e\,e^{jm\theta}+\sum_{M=-\infty}^{\infty}[B_{Mpn}]^e[G_{mp}]^e\delta\{Y_{mp}\}^e\,e^{j(m+M)\theta}\right\} \tag{33}$$

Hence assuming that $\|\{Y_{mp}\}\|\ll 1$ for $s\epsilon S$, it follows that

$$(\delta\{\epsilon\}^e)^T\{\sigma\}^e\sim\sum_{m=-\infty}^{\infty}\sum_{M=-\infty}^{\infty}(\delta\{Y_{Mp}\}^e)^T\{[G_{Mp}]^T[B_{mpn}]^T[D]\{\epsilon_0\}+[[B_{Mp}]^T+[G_{Mp}]^T[B_{0n}]^T][D][B_{mp}]+[B_{0n}][G_{mp}]]\{Y_{mp}\}\}^e\,e^{j(m+M)\theta} \tag{34}$$

where $\{\epsilon_0\}$ represents the initial prestress strain field. By letting $\{\sigma_0\}$ represent the prestress state, the expression $[B_{mpn}]^T[D]\{\epsilon_0\}$ can be rewritten as follows

$$[B_{mpn}]^T[D]\{\epsilon_0\}=[\sigma^{(0)}][G_{mp}]\{Y_{mp}\} \tag{35}$$

where

$$[\sigma^{(0)}]=\begin{bmatrix}T_{10} & 0 & \tilde{T}_{120}\\ 0 & T_{10}+T_{20} & 0\\ \tilde{T}_{120} & 0 & T_{20}\end{bmatrix} \tag{36}$$

Therefore applying (35), (34) reduces to

$$(\delta\{\epsilon\}^e)^T\{\sigma\}^e\sim\sum_{m=-\infty}^{\infty}\sum_{M=-\infty}^{\infty}(\delta\{Y_{Mp}\}^e)^T[[G_{Mp}]^T[\sigma^{(0)}][G_{mp}]+[[B_{Mp}]^T+[G_{Mp}]^T[B_{0n}]^T][D]\times[[B_{mp}]+[B_{0n}][G_{mp}]]]^e\{Y_{mp}\}^e\,e^{j(m+M)\theta} \tag{37}$$

Now, performing the appropriate variational manipulations, in terms of (37), (27) yields the following finite element formulation

$$[[K_m]^e + \Omega^2[M_{m3}]^e]\{Y_{mp}\}^e + \Omega[M_{m2}]^e\{Y_{mp}\}^e_{,t} + [M_{m1}]^e\{Y_{mp}\}^e_{,tt} = \{0\} \tag{38}$$

such that

$$[K_m]^e = \int_{S_e} [[\bar{G}_{mp}]^T[\sigma^{(0)}][G_{mp}] + [[\bar{B}_{mp}]^T + [\bar{G}_{mp}]^T[B_{0n}]^T][D][[B_{mp}] + [B_{0n}][G_{mp}]]]^e r ds \tag{39}$$

and

$$[M_{mi}]^e = \int_{S_e} [N_m]^T[\alpha_i][N_m]\, r ds\,;\ i = 1, 2, 3 \tag{40}$$

For situations in which the initial prestress state is accompanied by small deflections, namely $\|\{Y_0\}\| \ll 1$ for $s \epsilon S$, the form of (39) can be simplified to yield

$$[K_M]^e \sim \int_{S_e} [[\bar{G}_{mp}]^T[\sigma^{(0)}][G_{mp}] + [\bar{B}_{mp}]^T[D][B_{mp}]]^e r ds \tag{41}$$

Unlike previous quasi-analytical developments, $[\sigma^{(0)}]$ represents the most general form of axisymmetric prestress field admissible. Furthermore, this is true regardless of whether moderate or small deflections are assumed.

Due to the symmetric and conjugate properties of $[G_{mp}]^e$ $[B_{mp}]^e$, $[\sigma^{(0)}]$ and $[D]^e$, it follows that $[K_m]^e$ is itself Hermitian in form, that is

$$([\bar{K}_m]^e)^T = [K_m]^e \tag{42}$$

Furthermore, due to (26),

$$[\bar{K}_m]^e = [K_{-m}]^e = ([K_m]^e)^T \tag{43}$$

This is true for both forms of $[K_m]^e$, namely that given by eqn (39) and that by eqn (41). Similarly, since $[\alpha_2]$ is skew symmetric and $[\alpha_3]$ is symmetric, it follows that $[M_{m2}]$ is Hermitian while for purely real $[N_m]$, $[M_{m1}]$ and $[M_{m3}]$ are both real and symmetric.

For the free vibration problem information concerning the properties of harmonic type oscillations is sought. Due to the appearance of even and odd ordered time derivatives in eqn (38), it follows that for the nonstationary case, $\{Y_{mp}\}^e$ must be taken in the form

$$\{Y_{mp}\}^e = \{\Gamma_{mp1}\}\, e^{j\omega_m t} + \{\Gamma_{mp2}\}\, e^{-j\omega_m t} \tag{44}$$

Hence, in terms of eqn (44), eqn (38) reduces to the following assembled complex regular matrix problem, namely

$$[[K_m] + \Omega^2[M_{m3}] \pm j\Omega\omega_m[M_{m2}] - \omega_m{}^2[M_{m1}]]\{\Gamma_{mp}(\pm j\omega_m)\} = \{0\} \tag{45}$$

For the nonstationary isotropic and orthotropic cases, it follows from eqn (45) that

$$\{\bar{\Gamma}_{mp}(j\omega_m)\} = \{\Gamma_{mp}(-j\omega_m)\} \tag{46}$$

In the more general fully anisotropic torque prestress case, because of the use of eqn (14), the transformed nodal displacements $\{\Gamma_{mp}\}$ satisfy the following complex conjugate properties

$$\{\bar{\Gamma}_{mp}(+j\omega_m)\} = \{\Gamma_{-mp}(-j\omega_{-m})\} \tag{47}$$

such that $\overline{j\omega_m} = -j\omega_{-m}$. Due to eqn (45) and (47), the eigenfunction associated with a given frequency eigenvalue is given by

$$\{Y_p\} = \{\Gamma_{mp}(j\omega_m)\} \exp(j(m\theta + \omega_m t)) + \{\bar{\Gamma}_{mp}(j\omega_m)\} \exp(-j(m\theta + \omega_m t)) + \{\Gamma_{mp}(-j\omega_m)\} \exp(j(m\theta - \omega_m t)) + \{\bar{\Gamma}_{mp}(-j\omega_m)\} \exp(-j(m\theta - \omega_m t)) \quad (48)$$

such that for stationary shells

$$\{Y_p\} = (\{\Gamma_{mp}\} e^{jm\theta} + \{\bar{\Gamma}_{mp}\} e^{-jm\theta}) \begin{pmatrix} \sin \omega_m t \\ \text{or} \\ \cos \omega_m t \end{pmatrix} \quad (49)$$

For the stability problem, eqn (38) reduces to:

(i) Moderate prestress deflections;

$$\int_S [[\bar{G}_{mp}]^T[\sigma^{(0)}][G_{mp}] + [[\bar{B}_{mp}]^T + [\bar{G}_{mp}]^T[B_{0n}]^T][D][[B_{mp}] + [B_{0n}][G_{mp}]]]r\,ds\{Y_{mp}\} = \{0\} \quad (50)$$

(ii) Small prestress deflections;

$$\int_S [[\bar{G}_{mp}]^T[\sigma^{(0)}][G_{mp}] + [\bar{B}_{mp}]^T[D][B_{mp}]]r\,ds\{Y_{mp}\} = \{0\} \quad (51)$$

In terms of either eqns (50) or (51), the eigenfunctions associated with a given stability problem take the form

$$\{Y_p\} = \{Y_{mp}\} e^{jm\theta} + \{\bar{Y}_{mp}\} e^{-jm\theta} \quad (52)$$

4. CRITICAL CIRCUMFERENTIAL TRAVELING WAVE EIGENVALUE PROBLEM

To establish the appropriate eigenvalue problem for the determination of the critical circumferential wave velocities, the Galilean coordinate transformation[18] is employed to convert eqn (27) to standing wave form. Since traveling waves induced by circumferentially moving surface tractions are considered, Fig. 2, the Galilean transform takes the form

$$\eta = \theta - \Omega^* t \quad (53)$$

where Ω^* represents the rotational speed of the tractions F_z and F_θ. In terms of eqn (53), eqn (27) reduces to

$$\int_{-\infty}^{\infty} \int_S ((\delta\{\epsilon\})^T\{\sigma\} + (\delta\{Y\})^T\{(\Omega^*)^2[\alpha_1]\{Y\}_{,\eta\eta} - \Omega\Omega^*[\alpha_2]\{Y\}_{,\eta} + \Omega^2[\alpha_3]\{Y\}\})r\,ds\,d\eta = 0 \quad (54)$$

Since $\eta\epsilon(-\infty,\infty)$, in order to obtain the proper η functional dependence for F_z, F_θ and the various

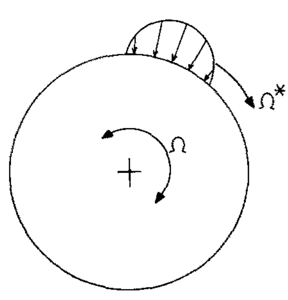

Fig. 2. Circumferentially moving surface tractions.

other field variables, the following bilateral Fourier integral representation is employed

$$\langle F_z, F_\theta, \{Y_p\}\rangle = \int_{-\infty}^{\infty} \langle F_{qz}, F_{q\theta}, \{Y_{pq}\}\rangle\, e^{-jq\eta}\, d\eta \tag{55}$$

such that

$$\langle F_{qz}, F_{q\theta}, \{Y_{pq}\}\rangle = (1/2\pi) \int_{-\infty}^{\infty} \langle F_z, F_\theta, \{Y_p\}\rangle\, e^{jq\eta}\, dq \tag{56}$$

Due to the inherent periodicity of the η space, it follows that

$$\langle F_{qz}, F_{q\theta}, \{Y_{pq}\}\rangle = \sum_{n=-\infty}^{\infty} e^{-jq2\pi n} \int_0^{2\pi} \langle F_z, F_\theta, \{Y_p\}\rangle\, e^{-jq\eta}\, d\eta \tag{57}$$

Hence, following[19], for all $\eta \epsilon\ (-\infty, \infty)$

$$\langle F_z, F_\theta, \{Y_p\}\rangle = \sum_{m=-\infty}^{\infty} \langle F_{mz}, F_{m\theta}, \{Y_{mp}\}\rangle\, e^{jm\eta} \tag{58}$$

where

$$\langle F_{mz}, F_{m\theta}, \{Y_{mp}\}\rangle = (1/2\pi) \int_0^{2\pi} \langle F_z, F_\theta, \{Y_p\}\rangle\, e^{-jm\eta}\, d\eta \tag{59}$$

In terms of eqns (15), (54) and (58), the wave shape $\{Y\}^e$ associated with F_z and F_θ for the given problem is taken in the form

$$\{Y\}^e \sim [N]^e\{Y_0\}^e + \sum_{m=-\infty}^{\infty} [N_m]^e\{Y_{mp}\}^e\, e^{jm\eta} \tag{60}$$

After the appropriate variational manipulations, eqn (54) reduces to the following complex linear eigenvalue problem, namely

$$[[K_m] + \Omega^2[M_{m3}] - j(m\Omega^*)[M_{m2}] - (m\Omega^*)^2[M_{m1}]]\{Y_{mp}\} = \{0\} \tag{61}$$

Comparing eqns (45) and (61), it follows that the critical velocities of the loads F_z and F_θ are directly related to the frequency eigenvalues by the relation $m\Omega^* = \omega_m$. Hence, there are an infinity of circumferential critical velocities which interestingly are independent of the distributional nature of the traveling surface tractions F_z and F_θ†. Furthermore, due to the general form of eqn (61), the foregoing is true both for moderate and small initial prestress deflection fields. The infinity of circumferential critical velocities noted above are in contrast with axially moving forces, which are known to excite only a finite number of critical wave speeds[20] (cylindrical shells), and which are not directly related to the frequency eigenvalues of the given structure.

5. EIGENFUNCTION AND EIGENVALUE PROPERTIES

Because of the inclusion of Coriolis forces, the pencil of (45) is a second order complex regular polynomial matrix. In order to establish some of the outstanding eigenvalue properties of the assembled counterpart of eqn (45), premultiplication by $[\bar{\Gamma}_{mp}]$ yields the following quadratic form

$$(\{\bar{\Gamma}_{mp}\})^T\, [[K_m] + \Omega^2[M_{m3}] + j\Omega\omega_m[M_{m2}] - \omega_m^2[M_{m1}]]\, \{\Gamma_{mp}\} = \{0\} \tag{62}$$

Solving eqn (62) for ω_m yields the following generalized version of Rayleigh's quotient, namely

$$\omega_m = \frac{jM^*_{m2} \pm \sqrt{((jM^*_{m2})^2 + 4K^*_m)}}{2M^*_{m1}} \tag{63}$$

†So long as F_z and F_θ are moderate loads.

where M^*_{m1}, M^*_{m2} and K^*_m represent the following quadratic forms;

$$M^*_{m1} = (\{\bar{\Gamma}_{mp}\})^T[M_{m1}]\{\Gamma_{mp}\} \tag{64}$$

$$M^*_{m2} = \Omega(\{\bar{\Gamma}_{mp}\})^T[M_{m2}]\{\Gamma_{mp}\} \tag{65}$$

$$K^*_m = (\{\bar{\Gamma}_{mp}\})^T[[K_m] + \Omega^2[M_{m2}]]\{\Gamma_{mp}\} \tag{66}$$

Since $j[M_{m2}]$ is Hermitian, the quadratic form $j\Omega[\bar{\Gamma}_{mp}][M_{m2}]\{\Gamma_{mp}\}$ is itself purely real. Hence, for a positive discriminant, it follows from (63) that Coriolis forces induce a two fold bifurcation of the frequency eigenvalue branches of general shells of revolution. Such bifurcations are about the branches of the stationary case. Since $[K_m]$ has not been specialized, this result applies both for the moderate and small prestress deflection situations. For the stationary case ($\Omega = 0$), (63) reduces to the more traditional form

$$\omega_m{}^2 = [\bar{\Gamma}_{mp}] \int_S [[\bar{G}_{mp}]^T[\sigma^{(0)}][G_{mp}] + [[\bar{B}_{mp}]^T + [\bar{G}_{mp}]^T[B_{0n}]^T][D] \times [[B_{mp}] + [B_{0n}][G_{mp}]]]r\,ds\{\Gamma_{mp}\}/(\{\bar{\Gamma}_{mp}\})^T[M_{m1}]\{\Gamma_{mp}\} \tag{67}$$

A further implication of this result is that Coriolis forces also cause a two-fold bifurcation in the total number of critical circumferential traveling wave velocities. This follows directly from analyzing the Rayleigh quotient of eqn (61).

The gross effects of the various forms of $[\sigma^{(0)}]$, $[M_{m1}]$. $[M_{m3}]$ and $[D]$ can be forecasted from eqns (63) and (67) via the use of the classical Courant–Fischer theorem[21]. For example, for a purely tensile prestress field $[\sigma^{(0)}]$ is positive definite, hence via Courant–Fischer obviously all the frequency eigenvalues are raised compared to the prestress free set. In the case of a shear type prestress field, due to the indefiniteness of $[\sigma^{(0)}]$, the frequency eigenvalues may lie above and below the prestress free case. This of course leads to the possibility of bifurcations in the eigenvalue spectrum. Similar comments can also be made concerning the effects of $[M_{m2}]$, $[M_{m3}]$, and the anisotropic elements of $[D]$ which all have inherently indefinite quadratic forms.

In order to establish the orthogonality properties of $\{\Gamma_{mp}\}$, assume that there exists distinct eigenvalues (ω_{ma}, ω_{mb}) which respectively satisfy†

$$[[K_m] + \Omega^2[M_{m3}] + j\Omega\omega_{ma}[M_{m2}] - \omega^2_{ma}[M_{m1}]]\{\Gamma_{mpa}\} = \{0\} \tag{68a}$$

$$[[K_m] + \Omega^2[M_{m3}] + j\Omega\omega_{mb}[M_{m2}] - \omega^2_{mb}[M_{m1}]]\{\Gamma_{mpb}\} = \{0\} \tag{68b}$$

Now subtracting the results of the premultiplication of (68a) by $[\bar{\Gamma}_{mpb}]$ yields the following unusable form of orthogonality condition, namely

$$(\omega^2_{mb} - \omega^2_{ma})(\{\bar{\Gamma}_{mpb}\})^T[M_{m1}]\{\Gamma_{mpa}\} - j\Omega(\omega_{mb} - \omega_{ma})(\{\bar{\Gamma}_{mpb}\})^T[M_{m2}]\{\Gamma_{mpa}\} = 0 \tag{69}$$

For the stationary case ($\Omega \equiv 0$), eqn (69) reduces to the more traditional form

$$(\{\bar{\Gamma}_{mpb}\})^T[M_{m1}]\{\Gamma_{mpa}\} = 0 \tag{70}$$

As with the generalized and specialized Rayleigh quotients, (63) and (67), the orthogonality relations eqns (69) and (70) differ from those of the stationary, torsionless orthotropic case in that $[K_m]$, $\{\Gamma_{mp}\}$ etc. are intrinsically complex. This complexity is directly due to the effects of torque prestress and Coriolis forces as well as material anisotropy. Hence, the deletion of any two of these effects still leads to complex equations whose pencils are inherently Hermitian.

6. DISCUSSION

For the frequency eigenvalue problem $[K_m]$ is inherently Hermitian.‡ Thus, for $\Omega \neq 0$, eqn (45) represents a complex 2nd order regular polynomial matrix problem. Hence, eqn (45) can be

†Consider that the discrimiant of eqn (63) is positive definite.
‡This follows regardless of whether moderate or small deflection fields are considered.

recast as the following complex linear eigenvalue problem[21], namely

$$\left[\begin{bmatrix} 0 & [K_m]+\Omega^2[M_{m3}] \\ [K_m]+\Omega^2[M_{m3}] & j\Omega[M_{m2}] \end{bmatrix} - \omega_m \begin{bmatrix} [K_m]+\Omega^2[M_{m3}] & 0 \\ 0 & [M_{m1}] \end{bmatrix}\right] \begin{Bmatrix} \Gamma_{mp} \\ \omega_m \Gamma_{mp} \end{Bmatrix} = \{0\} \quad (71)$$

Since the pencil of (71) is complex, the eigenvalue procedure recently developed by Gupta[17] can be used to evaluate ω_m. For stationary situations, eqn (45) degenerates to

$$[[K_m] - \omega_m{}^2[M_{m1}]]\{\Gamma_{mp}\} = \{0\} \quad (72)$$

for which Gupta's procedure must still be employed. This is due to the Hermitian nature of $[K_m]$ which is a direct outgrowth of the material anisotropy and torque prestress admitted herein.

In the case of stability problems, the eigenvalues of

$$\left[\int_S [\bar{B}_{mp}]^T[D][B_{mp}]r\,ds + \Omega^2[M_{m3}] + [K_{mn}(\lambda)]\right]\{\Gamma_{mp}\} = \{0\} \quad (73)$$

can be found by the "plotting procedure" a la Almroth and Bushnell[22]. Here of course, in contrast to[22], since $[K_m]$ is Hermitian its determinant is a complex constant for inappropriate eigenvalue parameters λ. In general, in all the numerical experiments performed for this study, $Re(det[K_m])$ and $Im(det[K_m])$ approach zero simultaneously for the appropriate λ. Hence, for simplicity, the "plotting" procedure can be employed by monitoring only $Re(det[K_m])$. Alternatively, the iterative technique developed by Cohen[2], and subsequently employed by Bushnell[4], can be generalized for use here. Such a procedure involves a sequence of eigenvalue problems that converges to the actual load state for which $det[K_m] = 0$. A typical eigenvalue problem in the sequence is

$$\left[\left[\int_S [\bar{B}_{mp}]^T[D][B_{mp}]r\,ds + [K_{mn}] + \Omega^2[M_{m3}] + \lambda_k[K_{mn}]\right]\right]\{\Gamma_{mp}\} = \{0\} \quad (74)$$

where λ_k is the kth correction of the kth load state, namely

$$\{F_s, F_\theta, F_z\}_{k+1} = \{F_s, F_\theta, F_k\}_k(1+\lambda_k) \quad (75)$$

In terms of (75), the iteration procedure is continued until λ_k reaches some preassigned limit. The main difference here is that $[K_m]$ is inherently Hermitian rather than real and asymmetric as in traditional analyses employed for orthotropic stationary shells subject to torsionless prestress states.

As noted earlier, because of the use of complex series expansions, namely eqn (16), the intraelement and nodal displacements are inherently complex, such that the transformed fields must satisfy the conjugate properties noted by eqn (26). In order to retain the demonstrated capabilities of the shape functions used in previous axisymmetric analyses, for this study, $[N]$ are chosen as real functions of the meriodional variable s such that the actual functional families used are identical to those employed in previous orthotropic studies. In terms of such a development, the entire complexity therefore resides in the transformed nodal displacements $\{Y_{mp}\}$, wherein $Re(\{Y_{mp}\})$ and $Im(\{Y_{mp}\})$ are coupled due to Coriolis, anisotropy and torque prestress effects.

To illustrate the potential of the quasi-analytical finite element procedure developed herein, the results of several numerical experiments are presented in this section:

(i) *Torque buckling of isotropic cylinders.* Donnell's early approximate solution for torque buckling of cylinders has been improved by several investigations. Of these, the most accurate available solutions were reported by Yamaki and Kodama[23] and Budiansky[24]. Figure 3 presents a comparison of results on cylinder torque buckling for a wide range of shell geometries and for the freely and clamped supported cases. The element type used to perform the numerical calculations had the form of the usual straight line variety with the exception that, as noted earlier, the nodal displacements were treated as complex. Furthermore in keeping with traditional

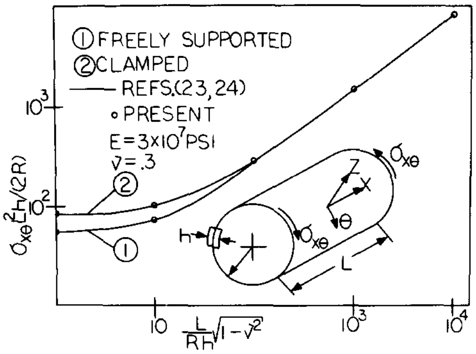

Fig. 3. Torsional buckling of isotropic cylinders.

torque buckling procedures, the prestress field was considered as a purely membrane state. Although, a "small" word size IBM 370-155 was employed to perform most of the computations, good accuracy was achieved over most of the range of variables considered. For $\sigma_{x\theta}^{(0)} \sim 0$ ($\sigma_{x\theta}$ crit.), a strong coupling between $Re(\{Y_{mp}\})$ and $Im(\{Y_{mp}\})$ was revealed. This coupling resulted in the spiraling mode shape typical of torque buckling.

(ii) *Stability of prestress anisotropic cylinders.* Figures 4 and 5 present a comparison of results for an anisotropic sandwich cylinder subject to torque or radial prestress. As in (i), the element type used to obtain the numerical results consisted of the straight line variety. For both the stability problems considered, as in traditional treatments, the prestress fields were considered as linear membrane states. In addition to illustrating the essential agreement between the "exact" [25] and element generated results, the significant effects of material and constructional anisotropy are also revealed. Furthermore, similar to the torque prestress case treated in (i), anisotropy induced a strong coupling between $Re(\{Y_{mp}\})$ and $Im(\{Y_{mp}\})$ which also resulted in a spiraling type mode shape.

(iii) *Torque prestress and Coriolis effects on frequency and critical circumferential wave velocity spectrums of clamped rotating cylinders.* The comparison illustrated in Fig. (6) considers

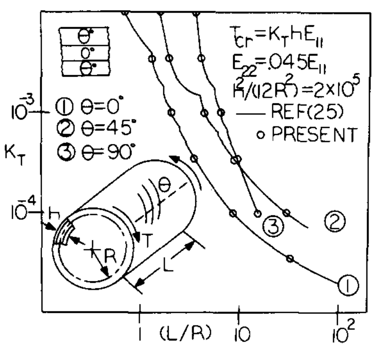

Fig. 4. Buckling of clamped anisotropic sandwiched cylindrical shells subject to torque.

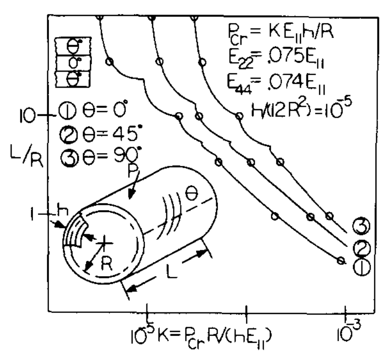

Fig. 5. Buckling of freely supported anisotropic sandwiched cylindrical shell subject to external pressure.

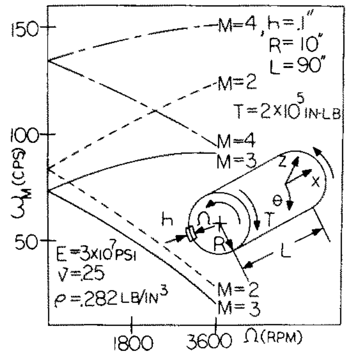

Fig. 6. Effects of rotational speed on frequency eigenvalues of torque prestress clamped cylinder.

the effects of torque prestress and Coriolis forces on the frequency eigenvalues of rotating cylinders. The exact results presented in these figures for comparison purposes were obtained by employing the analytical procedure recently described in[9]. Since the numerical results presented in[9] were restricted to the infinite case, in order to reveal the effects of torque prestress and Coriolis forces on cylinders with end contraints, this work considers clamped boundaries. As in the infinite case, for clamped boundaries significant bifurcations in the frequency eigenvalue spectrum continue to be induced by Coriolis forces. By interpreting ω_m appropriately, Fig. 6 can also be used to glean information concerning the effects of Ω and T on Ω^*.

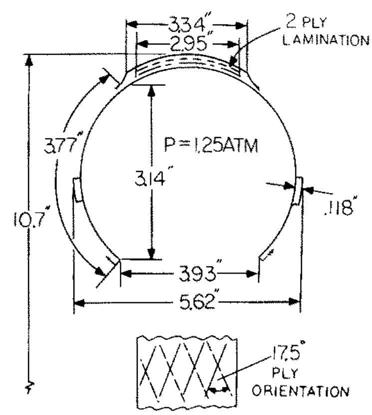

Fig. 7. Geometry of laminated toroidal configuration.

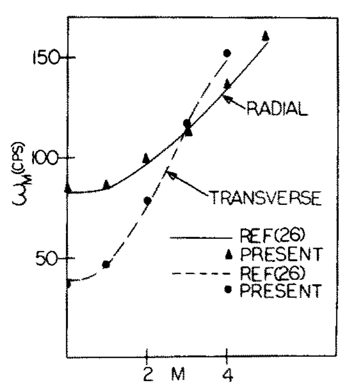

Fig. 8. Frequency eigenvalues of pressurized freely supported laminated toriodal configuration (Fig. 7).

(iv) *Frequency eigenvalues of a pressurized laminated toriodal shell configuration.* Considering the tire like reinforced rubber shell configuration described in Fig. 7, Fig. 8 presents a comparison of element and experimentally generated results[26]. The shape function used for this study consisted of the Giannini and Miles[27] curved element approximation. Although adequate representation was obtained, the main difference in the results presented can be attributed to the lack of adequate material characterization[26] and shell geometry description.

SUMMARY

The capabilities of the quasi-analytical finite element procedure for shells of revolution has been extended to handle free vibration and stability problems incorporating:

(i) Coriolis acceleration loads;
(ii) General axisymmetric prestress states including torque loads;
(iii) Material and/or structurally induced anisotropy.

Because of the form of the solution procedure employed herein, several presently available general and special purpose finite element computer codes (SAP, etc.) can be updated to include such capabilities. Furthermore, due to the inherent generality of the solution form employed, the finite difference approach of Bushnell[4], (BOSOR series codes), can also be updated to incorporate the above noted effects.

REFERENCES

1. P. E. Grafton and D. R. Strome, Analysis of axisymmetrical shell by the direct stiffness method. *AIAA J.*, **1**, 2342 (1963).
2. G. A. Cohen, Computer analysis of asymmetric buckling of ring stiffened orthotropic shells of revolution. *AIAA J.*, **6**, 2305 (1968).
3. A. Kalnins, Static, free vibrations and stability of thin elastic shells of revolution. Report AFFDL-TR-68-144, Air Force Flight Dynamics Laboratory, Wright–Patterson Air Force Base, Ohio (1969).
4. D. Bushnell, Analysis of buckling and vibration of ring-stiffened, segmented shells of revolution. *Int. J. Solids and Structures.* **6**, 157 (1970).
5. B. H. Gallagher and T. Y. Yang, Elastic instability predictions for doubly curved shells. *Proc. 2nd Conf. Matrix Methods In Structural Mechanics*, TR-68-150, pp. 711–739. Air Force Dynamics Lab, Wright–Patterson Air Force Base, Ohio Dec. (1969).
6. T. Y. Yang and H. W. Kim, Vibration and buckling of shells under initial stress. *AIAA J.*, **11**, 1525 (1973).
7. C. W. Bert, J. L. Baker and D. M. Egle, Free vibrations of multilayer anisotropic cylindrical shells. *J. Composite Materials*, **3**, 480 (1969).
8. J. Padovan, Frequency and buckling eigenvalues of anisotropic cylinders subjected to nonuniform lateral prestress. *Int. J. Solids and Structures.* **7**, 1449 (1971).
9. J. Padovan, Natural frequencies of rotating prestressed cylinders. *J. Sound and Vibrations.* **31**, 469 (1973).
10. L. R. Koval and E. T. Cranch, On the free vibration of thin cylindrical shells subjected to an initial static torque. *Proc. 4th U.S. Nat. Congr. Appli. Mech.* Vol. 1, pp. 107–117 (1962).
11. A. V. Srinviasan and C. F. Lauterbach, Traveling waves in rotating cylindrical shells. *J. Engrg for Industry*, **91**, 1129 (1971).
12. L. Penzes and H. Kraus, Free vibration of prestressed cylindrical shell having arbitrary homogeneous boundary conditions. *AIAA J.* **10**, 1309 (1972).
13. W. Soedel, On the dynamic response of the rolling tire. *8th Int. Cong. Acoustics, London, July*, pp. 23–31 (1974).
14. W. F. Ames, Waves in tires. *Textile Research Journal*, **40**, 498 (1970).
15. V. V. Novoshilov, *The theory of thin shells.* Chap. 1. Noordhoff, Groningen (1959).
16. J. Padovan, Quasi-analytical finite element procedure for axisymmetric anisotropic shells and solids. *J. Computers and Structures*, **4**, 467 (1974).
17. K. K. Gupta, Free vibration analysis of spinning structural systems. *Int. J. Num. Meth. Engrg.*, **5**, 395 (1973).
18. C. Sve and G. Herrmann, Moving load on a laminated composite. *J. of Applied Mech.* **41**, Serrest, No. 3, 663 (1974).
19. A. Papoulis, *The Fourier Integral and Its Applications.* pp. 42–47. McGraw-Hill, New York (1962).
20. K. Schiffner and C. R. Steele, Cylindrical shell with an axisymmetric moving load. *AIAA J.* **9**, 37 (1971).
21. P. Lancaster, *Theory of Matrices.* pp. 115–119. Academic Press, New York, (1969).
22. B. O. Almroth and D. Bushnell, Computer analysis of various shells of revolution. *AIAA J.* **6**, 1848 (1968).
23. N. Yamaki and S. Kodama, Buckling of circular cylinder shells under torsion. Report 2, *Rep. Inst. High Sp. Mech. Japan*, Vol. 18, pp. 121–142 (1966/1967).
24. B. Budiansky, Post buckling behavior of cylinders in torsion. *IUTAM Symposium, Copenhagen* 1967, *Proc. Theory of Thin shells.* (Edited by F. I. Niordson) Springer-Verlag, Berlin (1969).
25. B. P. C. Ho and S. Cheng, Some problems in stability of heterogeneous aeolotropic cylindrical shells under combined loadings. *AIAA J.* **1**, 1603 (1963).
26. F. Böhm, Mechanics of the belted tire. Transl., No. 5, ORA Project 02957, The University of Michigan, (Feb. 1967).
27. M. Giannini and G. A. Miles, A curved element approximation in the analysis of axisymmetric thin shells. *Int. J. Num. Meth. in Eng.* **2**, 459 (1970).

APPENDIX

$$[B_{mi}]^e = \begin{bmatrix} \frac{r}{R_2} N'_{mi} & r' N'_{mi} & 0 \\ 0 & \frac{1}{r} N_{mi} & j\frac{m}{r} N_{mi} \\ j\frac{m}{R_2} N_{mi} & j\frac{mr'}{r} N_{mi} & N'_{mi} - \frac{r'}{r} N_{mi} \\ (r' N'_{mi})' & -\left(\frac{r}{R_2} N'_{mi}\right)' & 0 \\ \frac{(r')^2}{r} N'_{mi} - \left(\frac{m}{r}\right)^2 r' N_{mi} & \frac{m^2}{rR_2} N_{mi} - \frac{r'}{R_2} N'_{mi} & j\frac{m}{rR_2} N_{mi} \\ jm\left(\left(\frac{r'}{r}\right) N'_{mi} - \left(\frac{r'}{r}\right)^2 N_{mi}\right) & jm\left(\frac{r'}{rR_2} N_{mi} - \frac{1}{R_2} N'_{mi}\right) & \left(\frac{1}{R_1} N'_{mi} - \frac{r'}{rR_2} N_{mi}\right) \end{bmatrix}^e$$

$$[G_{mpi}]^e = \begin{bmatrix} r' N'_{mi} & -\frac{r}{R_2} N'_{mi} & 0 \\ j\frac{m}{R_2} N_{mi} & jm\frac{r'}{r} N_{mi} & \frac{r'}{r} N_{mi} \\ -jm\frac{r'}{r} N_{mi} & j\frac{m}{R_2} N_{mi} & \frac{1}{R_2} N_{mi} \end{bmatrix}^e$$

$$\chi_0 = \sum_{l=i,k,\dots} (r' N'_l \xi_{0l} - (r/R_2) N'_l \eta_{0l})$$

$$\beta_0 = (r'/r) \sum_{l=i,k,\dots} N_l v_{0l}$$

$$\psi_0 = (1/R_2) \sum_{l=i,k,\dots} N_l v_{0l}$$

$$\chi_{mp} = \sum_{l=i,k,\dots} (r' N'_{ml} \xi_{mpl} - (r/R_2) N'_{ml} \eta_{mpl})$$

$$\beta_{mp} = \sum_{l=i,k,\dots} ((r'/r) N_{ml} v_{mpl} + jm((1/R_2) N_{ml} \xi_{mpl} + (r'/r) N_{ml} \eta_{mpl}))$$

$$\psi_{mp} = \sum_{l=i,k,\dots} ((1/R_2) N_{ml} v_{mpl} + jm((1/R_2) N_{ml} \eta_{mpl} - (r'/r) N_{ml} \xi_{mpl}))$$